Journal of Theoretical and Applied Mechanics, Sofia, 2008, vol. 38, Nos 1–2, pp. 25–44

NUMERICAL MODELLING OF COUPLED MECHANICS AND GAS TRANSFER AROUND RADIOACTIVE WASTE IN LONG-TERM STORAGE*

P. Gerard, R. Charlier
Université de Liège, ArGEnCo, Chemin des Chevreuils, 1 – 4000 Liège, Belgium,
e-mails: pgerard@ulg.ac.be, Robert.Charlier@ulg.ac.be

J.-D. Barnichon, K. Su
Agence nationale pour la gestion des déchets radioactifs (ANDRA), France

J.-F. Shao, G. Duveau
Laboratoire de Mécanique de Lille, Université de Lille, France

R. Giot
Laboratoire Environnement, Géomécanique et Ouvrages,
Ecole Nationale Supérieure de Géologie de Nancy, France

C. Chavant
EDF, France

F. Collin
Université de Liège, ArGEnCo, Chemin des Chevreuils, 1 – 4000 Liège, Belgium,
FNRS Research Associate,
e-mail: f.collin@ulg.ac.be

[Received 10 October 2007. Accepted 25 February 2008]

Abstract. During long-term storage of radioactive waste, steel containers will be corroded. This process leads to hydrogen production. A boundary value problem has been proposed to study the numerical modelling of the gas migration and its coupling with the mechanical strains and stresses, under isothermal conditions. Biphasic fluid transfer model (considering water, vapour, gaseous hydrogen and dissolved hydrogen) is defined. A 2D axisymmetric case with simplified geometry close to waste disposal in clay is modelled. Fluid transport problem is first resolved. Then, coupled mechanics and fluid transfers are modelled to determine the coupling effects.
Key words: numerical modelling, gas transfer, radioactive waste, hydro-mechanical coupling, two-phase flow model.

*The authors would like to thank ANDRA and the FRS-FNRS for their financial support.

1. Introduction

In the frame of nuclear waste disposal, the numerical modelling of the underground facilities construction is used to simulate the different physical processes occurring during the live-time of the nuclear waste. The final objective of the design is the following: the host formation and the engineered barrier systems must be as impervious as possible in order to preserve the biosphere from the radionuclides migration. The Thermo-Hydro-Mechanical modelling needs numerical codes able to tackle this highly coupled problem. In most cases, these numerical computations are achieved under the assumption of constant gas pressure. However, after the introduction of the waste canisters, different potential gas sources exist in the storage gallery [1, 2]. The main origin of the gas is the corrosion of canister steel component. In this latter case, hydrogen is mainly produced and it is thus important to study how the gas will diffuse in the host formation. Indeed gas overpressure can maybe have a negative impact on the design. The gas transfer has been studied experimentally [2, 3], exhibiting complex behaviour especially for initially water saturated conditions. Tests showed that gas entry and breakthrough are often accompanied by the development of preferential pathways, which propagate through the sample. In this latter case, initial soil heterogeneity can provide an explanation for the preferential flow [4]. However, preferential pathways simulation is not under the scope of this paper. The idea is to study the gas-mechanical coupling effect, using a mechanical model and a two-phase flow model within a Biot theory framework. The boundary value problem modelled in this paper comes from a benchmark exercise, which has been organised with the following partners: University of Liège, Laboratory of Mechanics of Lille, Ecole Nationale Supérieure de Géologie de Nancy and EDF. The objective of the benchmark is to check the ability of different finite element codes to simulate the physical processes. The proposed exercise contents the major features of a repository (storage gallery, bentonite plug, etc.) but the geometry and the constitutive models are as simple as possible because the final goal of the benchmark is the check of numerical codes and not to study in detail the storage design. Each partner uses the same governing equations, but different finite element codes. The numerical implementation is thus possibly different (time integration, coupling terms, etc.). The objective of this paper is not to evidence the different numerical strategy of each team (the numerical solutions given by the partners are actually satisfactory similar). The purpose of the paper focuses on the different physical processes to be modelled and the coupling phenomena occurring within the considered simplified problem.

In section 2, the boundary value problem of the benchmark is described. A bi-dimensional axisymmetric modelling is proposed with some symmetry assumptions in order to limit the dimensions of the problem. The two-phase flow model and the mechanical model are defined, respectively, in section 3 and 4. In section 5, the results of the exercise are presented.

2. Boundary value problem

The geometry of the problem is based on a high-level and long-lived radioactive waste repository in argillite [5, 6], limited to a storage gallery and an access gallery (Fig. 1). Upper part of the domain is confined by argillite layer. Symmetry revolution around the storage gallery axis is assumed (gravity is not taken into account) and lateral boundaries are defined by the symmetry axis of the repository.

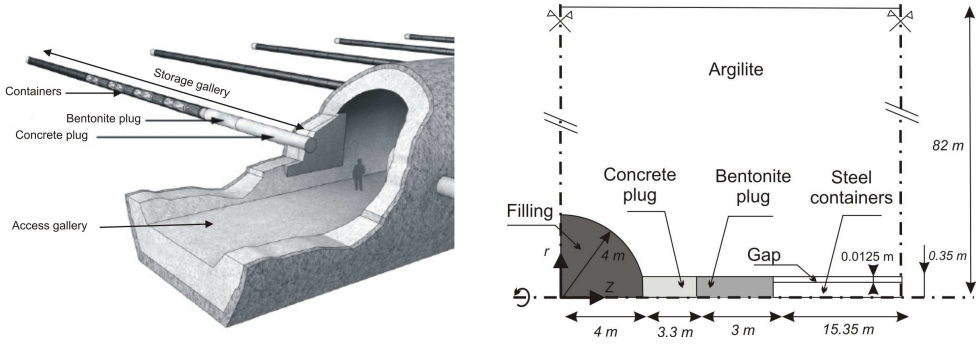

(a) (b)

Fig. 1. Schematic view of disposal gallery for high-level and long-lived radioactive waste (a) and geometry of the problem (b)

In this system, the bentonite and concrete plugs must restrict the transfers from the storage towards the gallery. The steel containers are not simulated and they are assumed rigid and impermeable. A gap existing between the containers and the gallery wall is modelled by a highly deformable porous medium.

Due to radioactive waste activity, heat is emitted over time and the conditions around the canisters are not isothermal. However, temperature variations are not taken into account for this modelling, because we focus our analysis on the coupling between the gas migration and the mechanical deformations. The introduction of thermal effects would affect the evolution of

the fluid pressures mainly due to thermal dilation. This will generate additional coupling effects, which will be studied in a future work.

2.1. Initial conditions

The initial conditions for the different materials are given in Table 1. For sake of simplicity, the stress state is assumed isotropic.

Table 1. Initial conditions in the different materials

Argilite	*Bentonite*	*Concrete*	*Filling*	*Gap*
$\sigma_0 = 12.3$ MPa	$\sigma_0 = 0.1$ MPa	$\sigma_0 = 0.1$ MPa	$\sigma_0 = 0.1$ MPa	$\sigma_0 = 0.1$ MPa
$p_w = 5$ MPa	$S_{r,w} = 0.80$	$p_w = 0.1$ MPa	$S_{r,w} = 0.80$	$S_{r,w} = 0.10$
$p_g = 0.1$ MPa	$p_g = 0.1$ MPa	$p_g = 0.1$ MPa	$p_g = 0.1$ MPa	$p_g = 0.1$ MPa
$T = 303$ °K	$T = 303$ °K	$T = 303$ °K	$T = 303$ °K	$T = 303$ °K

2.2. Boundary conditions

First the excavation of the storage and the access galleries is achieved for three days. Pore pressures and radial stresses at the galleries wall are decreased down to atmospheric pressure. Then a two-year rest period is imposed, during which water pressures are constant at the wall. During the second step, the bentonite, the concrete plug and the gap are introduced. A one-year resaturation phase of the plugs and the gap is then modelled, during which impervious condition and 50% relative humidity are imposed, respectively, along the containers and the access gallery wall. Radial displacements are fixed at the storage gallery wall. During these two first steps, the gas flow problem is not solved and gas pressure remains constant. Finally, during the third step, a hydrogen flow (corresponding to gas production due to containers corrosion) is injected in the radial direction from the steel containers into the argillite or the bentonite plug. Water impervious condition and fixed radial displacements are maintained at the storage gallery wall. At the access gallery wall, 50% relative humidity is imposed for 100 years, up to the placement of the filling in the access gallery. The total modelling time is 100 000 years and the temporal evolution of hydrogen flow imposed at containers wall is given by the following relationship:

$$
(1)\quad
\begin{array}{l}
\text{For } 2 < t \leq 4500 \text{ years: } V(t) = 9.969\ 10^{-11}\ \text{kg.s}^{-1}.\text{m}^{-2},\\
\text{For } 4500 < t \leq 20000 \text{ years: } V(t) = 1.495\ 10^{-11}\ \text{kg.s}^{-1}.\text{m}^{-2},\\
\text{For } 20000 < t \leq 50000 \text{ years: } V(t) = 9.969\ 10^{-13}\ \text{kg.s}^{-1}.\text{m}^{-2},\\
\text{For } t > 50000 \text{ years: } V(t) = 0.
\end{array}
$$

3. Biphasic flow model

To reproduce water and hydrogen flows in porous media, a biphasic flow model is used. In this latter model, two fluid phases are considered: a liquid and a gaseous one. The liquid phase is a mixture of liquid water and dissolved hydrogen. The gaseous mixture components are the water vapour and the gaseous hydrogen. Following the ideas of Panday [7] and Olivella [8], the fluid mass balance equations are written for each chemical species (i.e. water and hydrogen), and these read:

$$
(2)\quad \text{div}\left(\rho_w.\underline{q}_l + \underline{i}_v + \rho_v.\underline{q}_g\right) + \frac{\partial}{\partial t}\left(\rho_w.\phi.S_{r,w} + \rho_v.\phi.\left(1 - S_{r,w}\right)\right) - Q_w = 0,
$$

$$
\begin{aligned}
(3)\quad \text{div}\left(\rho_{H_2}.\underline{q}_g + \underline{i}_{H_2} + \rho_{H_2-d}.\underline{q}_l + \underline{i}_{H_2-d}\right)&\\
+ \frac{\partial}{\partial t}(\rho_{H_2-d}.\phi.S_{r,w} + \rho_{H_2}.\phi.\left(1 - S_{r,w}\right)) - Q_{H_2} &= 0,
\end{aligned}
$$

where $\underline{q}_l$ and $\underline{q}_g$ are the advection flows of liquid and gas phases (Darcy's law); $\underline{i}_v(= -\underline{i}_{H2})$ is the diffusion mass flows of vapour in the gaseous mixture and $\underline{i}_{H2-d}$ is the diffusion mass flows of dissolved hydrogen in liquid phase (Fick's law); Q_w and Q_{H2} are the sink terms of the different species; ϕ is the porosity; $S_{r,w}$ is the water relative saturation; ρ_i is the volumetric mass of the i constituent.

The diffusion mass flows (for a binary mixture of α and β components in a phase k (gaseous or liquid)) present a common form:

$$
(4)\qquad \underline{i}_\alpha = D^k_{\alpha-\beta}\underline{\nabla}\left(\frac{\rho_\alpha}{\rho_k}\right) = -\underline{i}_\beta,
$$

$D^k_{\alpha-\beta}$ is the diffusion coefficient of the component α in the phase k and ρ_k the volumetric mass of the phase. The expression of the diffusion coefficient is the following [9]:

$$D^k_{\alpha-\beta} = -\phi.S_{r,k}.\tau.\rho_k.D'^k_{\alpha-\beta}, \tag{5}$$

where τ is the tortuosity, $S_{r,k}$ is the relative saturation in the phase k and $D'^k_{\alpha-\beta}$ is the molecular diffusion coefficient of the component α in the phase k, depending on temperature and gas pressure [10].

The quantity of dissolved hydrogen is proportional to the quantity of gaseous hydrogen, due to Henri's law [10].

The water and hydrogen properties used in the biphasic flow model are given in Table 2.

Table 2. Water and hydrogen properties

μ_w	Water dynamic viscosity (Pa.s)	0.001
ρ_w	Water volumetric mass (kg.m^{-3})	1000
$1/\chi_w$	Water compressibility (Pa^{-1})	5 10^{-10}
$\mu^g_{H_2}$	Hydrogen dynamic viscosity (Pa.s)	9 10^{-6}
μ_v	Water vapour dynamic viscosity (Pa.s)	10^{-5}
$\rho^g_{H_2}$	Hydrogen volumetric mass (kg.m^{-3})	0.0794
H_{H_2}	Hydrogen Henri's coefficient $(-)$	0.0193
$D'^g_{H_2-H_2O}$	Molecular diffusion coefficient of the mixture of gaseous hydrogen and water vapour for $T = 303$ °K and $p_g = 101$ kPa (m^2.s^{-1})	9.5 10^{-5}
$D'^l_{H_2-H_2O}$	Molecular diffusion coefficient of dissolved hydrogen in liquid water for $T = 303$ °K and $p_g = 101$ kPa (m^2.s^{-1})	4.76 10^{-9}

The parameters of the different materials used in the biphasic flow model are given in Table 3.

The retention curve (Fig. 2) and the water and gas relative permeability functions of the different materials are given by the following relationships [12]. The gap relative permeability is considered constant and equal to one.

$$S_{r,w} = S_{res} + \frac{S_{\max} - S_{res}}{\left[1 + \left(\frac{p_c}{P_r}\right)^n\right]^m}, \tag{6}$$

Table 3. Hydraulic parameters for the different materials [6, 11]

		Argillite	Bentonite plug	Concrete plug	Filling	Gap
k_{int}^{sat}	Intrinsic permeability (m^2)	$2.75\ 10^{-20}$	$8\ 10^{-21}$	10^{-16}	$6\ 10^{-17}$	10^{-15}
Φ	Porosity (–)	0.18	0.366	0.15	0.33	1
m	Van Genuchten coefficient (–)	0.3289	0.3789	0.3507	0.2987	0.3333
n	Van Genuchten coefficient (–)	1.49	1.61	1.54	1.4203	1.5
P_r	Van Genuchten parameter (MPa)	15	16	2	0.12	0.05
$S_{\max}$	Maximal saturation (–)	1	1	1	1	1
S_{res}	Residual saturation (–)	0	0	0	0.1175	0
τ	Tortuosity (–)	0.25	0.0494	0.25	1	1

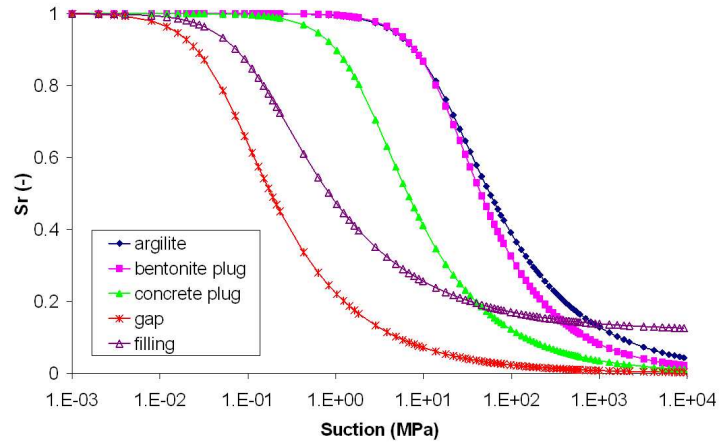

Fig. 2. Retention curves for the different materials

$$(7)\quad k_{r,w} = \sqrt{S_{r,w}}\left[1-\left(1-S_{r,w}^{1/m}\right)^{m}\right]^{2} \text{ and } k_{r,g} = \sqrt{1-S_{r,w}}\left[1-S_{r,w}^{1/m}\right]^{2m},$$

with $p_c(= p_g - p_w)$ the capillary pressure, $S_{\max}$ the maximal saturation, S_{res} the residual saturation, n and m the coefficients of van Genuchten's law with $m = 1 - 1/n$ and P_r a parameter of Van Genuchten's law.

4. Mechanical behaviour

For the considered materials and stress levels, the solid grain deformability is no more negligible and the general Biot framework [13] is used to model the hydromechanical coupled terms. Following the ideas of Biot, Coussy [14] proposed a thermodynamical framework of the problem, which leads to the expression of the porosity variation:

$$\dot{\phi} = (b - \phi).\left[\frac{S_{r,w}}{k_s}.\dot{p}_w + \frac{1 - S_{r,w}}{k_s}.\dot{p}_g + \frac{\dot{\Omega}}{\Omega}\right], \tag{8}$$

where p_w is the pore water pressure, p_g the gas pressure, b the Biot coefficient, $\dot{\Omega}/\Omega = \dot{\varepsilon}_V$ the skeleton volumetric deformation rate and k_s is the grain compressibility. The porosity variation is used in the fluid balance equations (equations (2) and (3)) in the computation of the storage term. It introduces a coupling term between the mechanical behaviour and the fluid transfers.

Mechanical behaviour of concrete, filling and gap is linear elastic. The mechanical law for argillite is an associated elastoplastic perfectly plastic model, defined by a Drucker-Prager yield surface. These constitutive models are written in terms of the Bishop's definition of effective stress [15]:

$$\sigma_{ij} = \sigma'_{ij} + b.\left(S_{r,w}p_w + (1 - S_{r,w})p_g\right)\delta_{ij}, \tag{9}$$

with σ'_{ij} the effective stress, and δ_{ij} the Kronecker symbol. This introduces a coupling term between the fluid transfers and the mechanical behaviour.

The generally observed behaviour of a compacted bentonite during wetting path is a reversible swelling for low stress level and a permanent collapse for high stress level [16]. The Barcelona Basic Model (BBM) [16] is a reference constitutive law for such material and is expressed in terms of the net stress and the suction. The bentonite considered for the disposal has a high value of preconsolidation pressure [5] and will encounter mainly elastic swelling during wetting paths. The model proposed for the bentonite is thus a simplified version of the BBM, considering only the nonlinear elastic behaviour described by the following relationship:

$$d\varepsilon_v^e = d\varepsilon_v^{e-m} + d\varepsilon_v^{e-s} = \frac{d\tilde{\sigma}_m}{K} + \frac{ds}{K_s}, \tag{10}$$

where $\tilde{\sigma}_m$ is the mean net stress, s is the suction, K is the bulk modulus and K_s is the bulk modulus related to suction changes.

The expression of the latter moduli is the following:

$$(11)\quad K(s) = K_0\left((1-r)\exp(-\beta s) + r\right) \text{ and } K_s(s) = K(s)\frac{1}{2\eta\beta_m}\frac{\exp\left(\beta_m s^2\right)}{(1+s)},$$

where $K_0(= E_0/3(1-2\nu_0))$ is the bulk modulus in saturated conditions, r (larger than unity), β, β_m and η are material parameters.

The mechanical parameters for the different materials are presented in Table 4.

Table 4. Mechanical parameters for the different materials [6, 11]

		Argillite	Bentonite plug	Concrete plug	Filling	Gap
E_0	Young modulus (MPa)	3271	150	30 000	38.46	0.1
υ_0	Poisson coefficient (–)	0.12	0.3	0.25	0.2	0.1
c	Cohesion (MPa)	3	–	–	–	–
φ	Friction angle (°)	15	–	–	–	–
r	Material parameter (–)	–	1.6	–	–	–
β	Material parameter (MPa^{-1})	–	200	–	–	–
η	Material parameter (MPa)	–	7	–	–	–
β_m	Material parameter (MPa^{-2})	–	0.0714	–	–	–
b	Biot coefficient (–)	0.6	1	0.8	1	1

5. Results

To highlight the potential effect of mechanical deformations on gas transfers, two modelling cases are considered. In the first case only the fluid transport problem is modelled and the medium is assumed infinitely stiff. In the second step, the coupling between fluids transfer and the mechanical behaviour is taken into account. The results are presented in different sections and also in terms of temporal evolutions in selected points (Fig. 3).

The numerical results are obtained with the LAGAMINE Finite Element code, developed in the University of Liège since the eighties. The detailed formulation of the THM coupled finite elements used for this modelling can be found in [17].

5.1. Fluid transport problem

In the first simulation, only water and hydrogen transfers are taken into account. The medium is infinitely stiff. First the results along the section C1

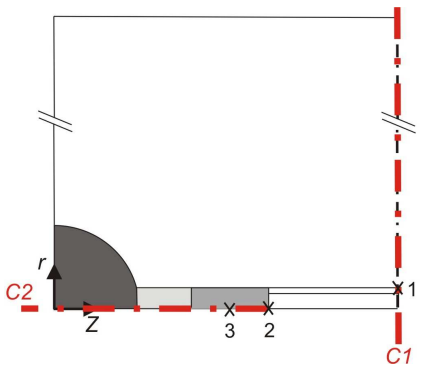

Fig. 3. Sections and points definitions for the results

are analysed. It makes possible the analysis of water and hydrogen exchanges in argillite and the influence of the gap. Then biphasic flows are analyzed in the bentonite and concrete plugs and near to the access gallery based on the results in the section C2.

In Figure 4, we present the gas and water pressures profiles along the section C1. Maximal gas pressure of about 7 MPa is reached at the wall and at the end of the first hydrogen injection phase (corresponding to 4500 years). When hydrogen injection decreases, gas pressure decreases also. At the end of the simulation (100 000 years), gas pressures have not recovered their initial values. The water pressures profiles show the argillite drainage during the first two years. Then the presence of the desaturated gap is considered and impervious condition is imposed at the wall. Water pressures increase at the wall. After 4500 years, water pressures recover the initial values and no water overpressure is observed in argillite. Considering the high permeability of the gap, gas pressures in argillite are not influenced by the presence of this gap and water and gas pressures are homogeneous in there.

Suction is maximum at the gallery wall and it is close to 2 MPa, which corresponds to a low desaturation in argillite according to the retention curve of this material. Figure 5(a) shows desaturation profiles in argillite (desaturation of the gap is not represented). Maximal desaturation is observed at the wall and it is about 1%. At the end of the first injection phase, the desaturation of argillite extends to 15 m (about 40 times the internal radius of the gallery).

Figure 5(b) presents dissolved and gaseous hydrogen flows profiles in comparison with saturation profiles along the section C1. In unsaturated zone, gaseous hydrogen is the most important, whereas this is dissolved hydrogen

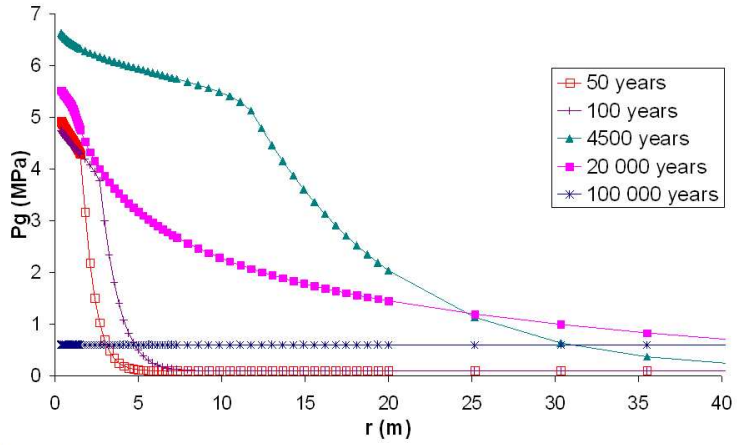

(a)

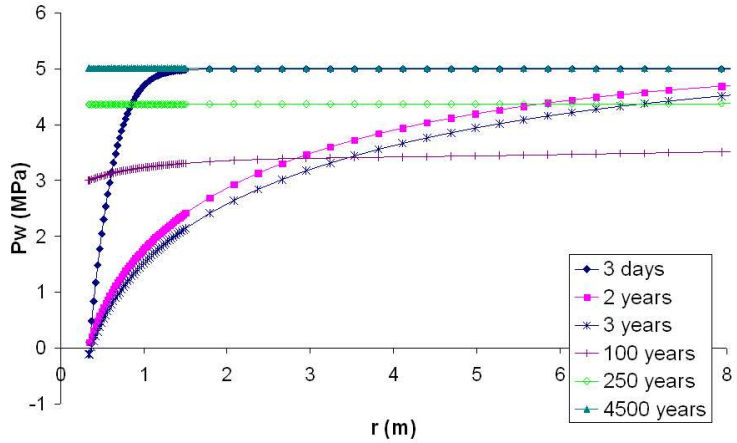

(b)

Fig. 4. Gas (a) and water (b) pressures profiles – Section C1

which plays essential role in the saturated zone. Indeed, for large hydrogen production, dissolved gas is not sufficient enough to transfer hydrogen (knowing that Henri's law limits dissolved hydrogen quantity) and a gaseous phase has thus to be created

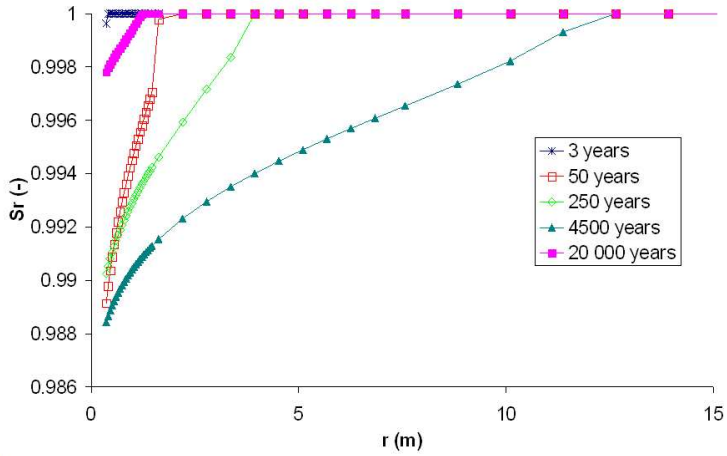

(a)

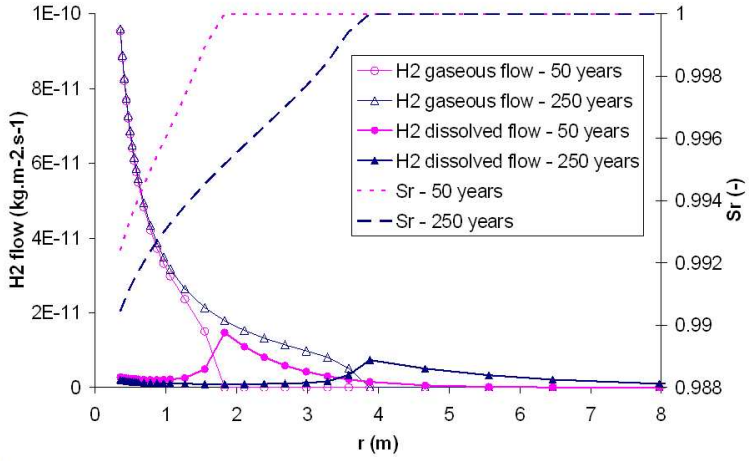

(b)

Fig. 5. Saturation profiles in argillite (a) and comparison between dissolved hydrogen and gaseous hydrogen flows (b) – Section C1

to inject hydrogen in argillite. Considering the axisymmetric conditions, gaseous hydrogen fluxes decrease with the radial distance. At the transition form unsaturated to saturated conditions, gaseous hydrogen has to be dissolved in the liquid phase. Maximum dissolved hydrogen fluxes are thus observed in the transition between saturated and desaturated zones.

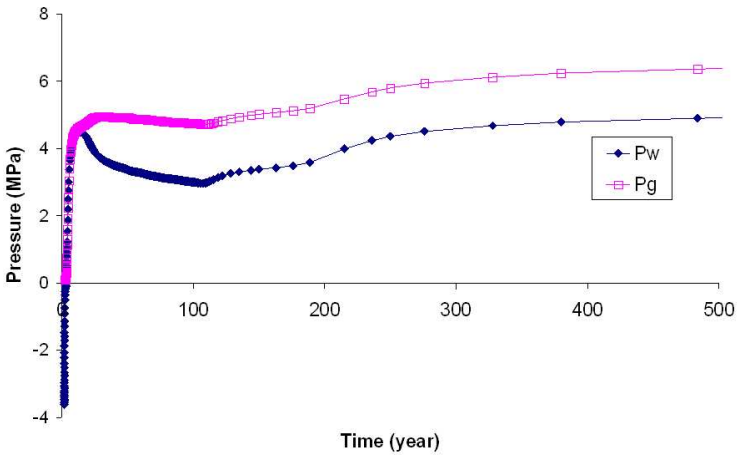

(a)

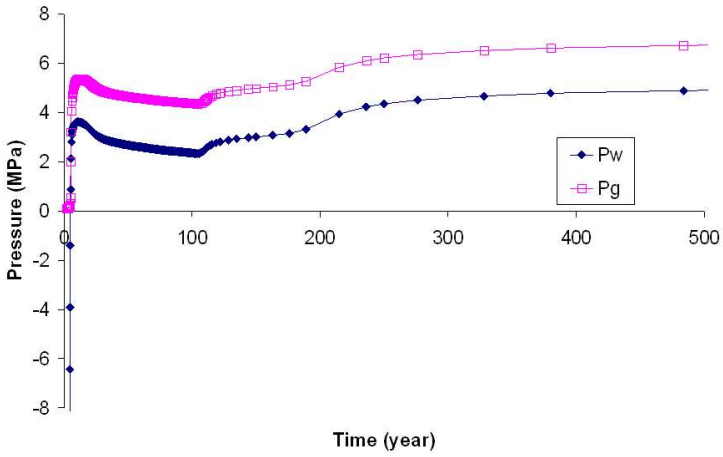

(b)

Fig. 6. Temporal evolution of water and gas pressures at points 1 (a) and 2 (b) as from 3 years

This analysis is confirmed by the temporal evolutions of water and gas pressures at point 1, located at the interface between the gap and the argillite. Figure 6(a) shows that gas pressures follow water pressures in order to maintain a constant suction (and thus a sufficient gas relative permeability) at the gallery wall. This suction comes as a result of the computation. It corresponds to gas saturation necessary for the injection of hydrogen.

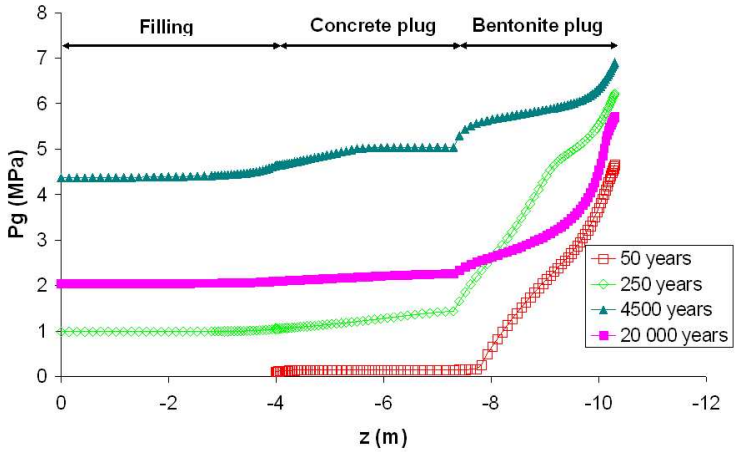

(a)

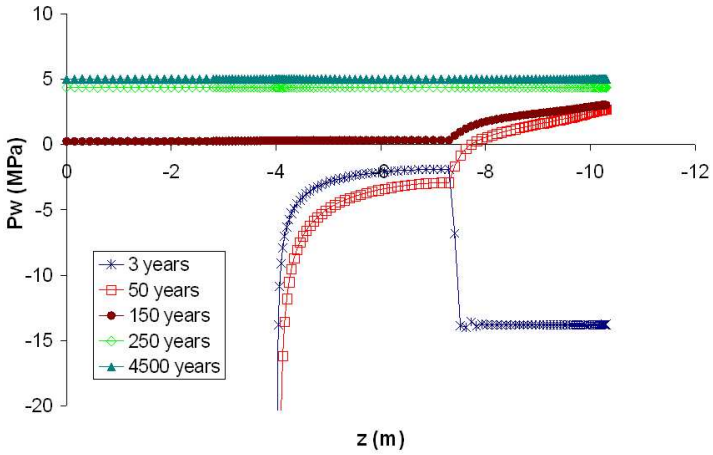

(b)

Fig. 7. Gas (a) and water (b) pressures profiles along C2

Pressure profiles in the engineered barrier along the section C2 are presented in Fig. 7. This section goes through the bentonite plug, the concrete plug and the filling. Figure 7(a) presents gas pressures profiles along C2. Gas pressures at the containers wall are influenced by water pressures in the way to maintain the suction constant. In the concrete plug and the filling, gas pressures distribution is relatively homogeneous, because of the high permeabilities of these two materials. Figure 6(b)

presents the temporal evolution of pressures at point 2, located in the interface between the containers and the bentonite. We observe a parallel evolution of water and gas pressures. The same phenomenon as in argillite (Fig. 6(a)) is thus observed.

Initially the bentonite plug is desaturated ($S_{r,w} = 0.80$ – $p_w = -13.85$ MPa) and water impervious condition is imposed at the bentonite – container contact. The bentonite plug is first resaturated. After 3 years, before the beginning of hydrogen injection, water pressures have not evolved significantly (Fig. 7(b)). When hydrogen injection begins, water pressure at the wall increases within 15 years. But progressively, the large drainage imposed at the access gallery wall (50% relative humidity corresponding to $p_w = -96$ MPa) affects, through the concrete plug, the water pressures in the bentonite plug. We observe thus a water pressure decrease first in the concrete and then in the bentonite (Figs 6(b) and 7(b)). Finally, after 100 years, filling is placed into the access gallery and drainage condition no longer holds. Water pressures increase and stabilize close to the initial value.

5.2. Coupled problem

In this simulation, the coupled effects of water and gas transfers on the mechanical behaviour (and of mechanical deformations on fluids transfer) are taken into account. The mechanical laws have been defined previously (section 4). After the excavation of galleries, a zone of plastic deformation is developed (referred as an Excavated Damage Zone (EDZ)). The extent of the EDZ is limited to the third of the internal radius. During hydrogen injection, the size of the EDZ does not evolve. Dilatancy effects appear thus in the argillite at the end of the excavation and water pressure profiles in there present thus negative values near to the gallery wall (Fig. 8(b)). Before 250 years, the increase of water pressures in argillite is delayed due to the coupling effects (storage term). After 250 years, there is no difference anywhere in terms of water pressures between the fluid transport and the coupled problems. As in the fluid transport problem, the gas pressures follow again the evolution of the water pressure. Before 250 years, the gas pressure profiles in the argillite are thus influenced by the hydro-mechanical coupling. After 250 years, the results are the same in the fluid transport and the coupled problems (Fig. 8(a)). The comparison between the fluid transport problem solution and the coupled problem solution in the different plugs along the section C2 shows also that the mechanical effects are limited on water and gas distributions (Fig. 9).

The analysis of the stresses in the different materials is also important. In particular temporal evolution of net stresses in the centre of the bentonite plug (point 3) is presented in Fig. 10(a). The evolution of net stresses has to be analyzed in function of the water and gas pressures at the same point (Fig. 10(b)). After the introduction of the bentonite plug, the resaturation is fast and a swelling pressure of 6 MPa is created. After 30 years, due to the hydrogen production, gas pressure increases progressively and through 50 years, one observes a re-desaturation of the bentonite due to gas production. The net stresses follow this evolution and decrease.

The effects of the mechanical behaviour on the gas transfer are thus limited. Plasticity in argillite or elastic nonlinear behaviour in bentonite do not influence significantly the gas evolution. The study of other strong coupled effects (permeability

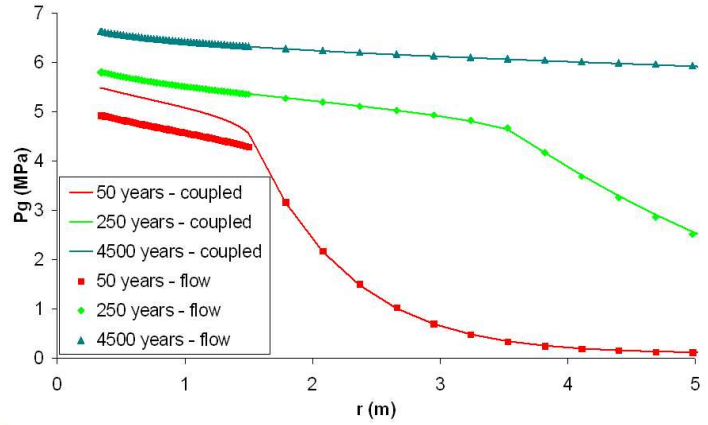

(a)

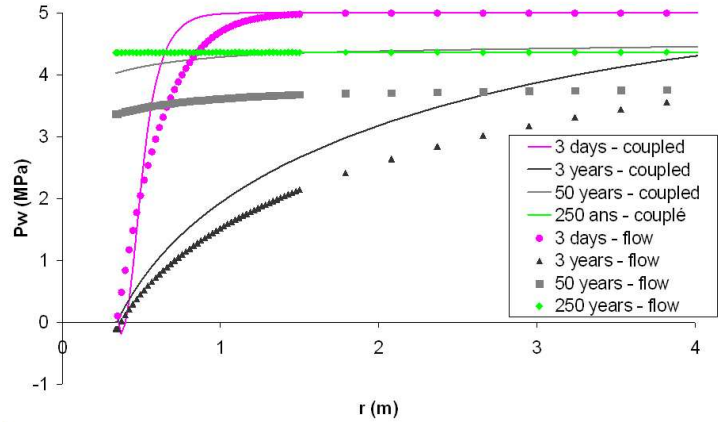

(b)

Fig. 8. Comparisons of gas (a) and water (b) profiles between flow and coupled simulations – Section C1

variation with damage, complex mechanical laws, retention curves evolution, etc.) can be interesting in the future.

6. Conclusions

During long-term storage of radioactive waste, steel containers will be corroded and this process will lead to hydrogen production. A boundary value problem

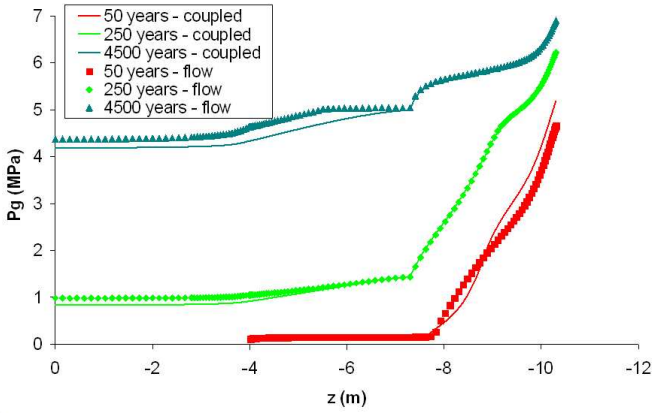

(a)

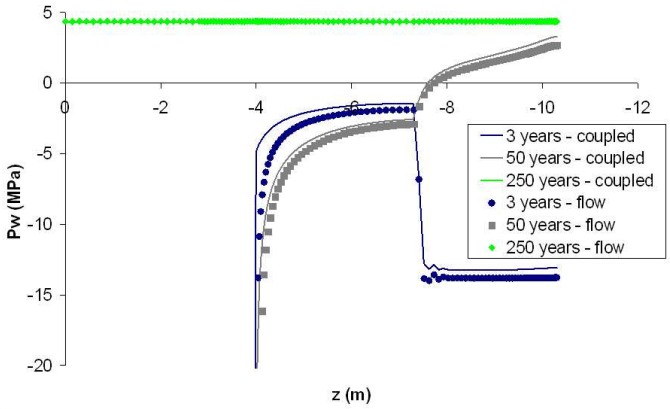

(b)

Fig. 9. Comparisons of gas (a) and water (b) profiles between flow and coupled simulations – Section C2

has been proposed to study the numerical modelling of the gas transfer and its coupling with the mechanical behaviour. The modelling has been done considering isothermal condition. Biphasic flow model (considering water, vapour, gaseous hydrogen and dissolved hydrogen) has been defined. A two dimensional axisymmetric case has been numerically studied with simplified geometry close to that of the waste disposal situated in clay. Fluid transport problem has been first resolved. Then, the couplings between fluid transfer and the mechanical behaviour have been modelled. Classical

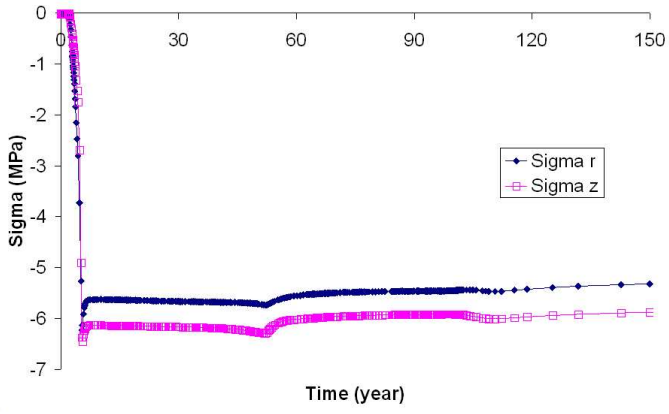

(a)

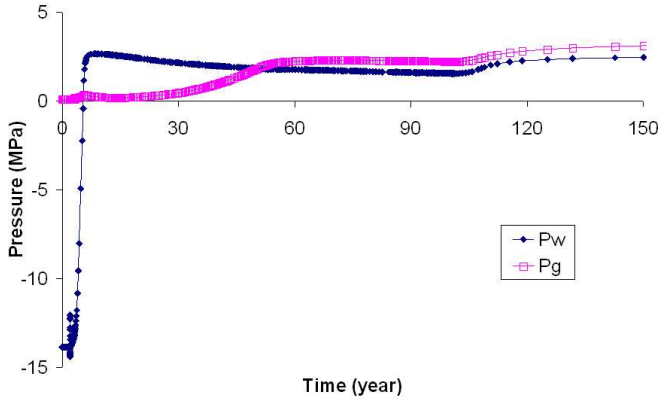

(b)

Fig. 10. Net stresses (a) and water and gas pressures (b) temporal evolution in bentonite – Point 3

mechanical laws (linear elasticity, nonlinear elasticity, elastic perfectly plastic with associated plasticity) have been used for the different materials.

The results show low desaturation of the argillite and of the bentonite plug. For large hydrogen production, dissolved gas is not sufficient enough to transport hydrogen (under Henri's law assumption) and a gaseous phase is created. Gaseous hydrogen flows are the most important in the unsaturated zone and the maxima of dissolved hydrogen flows are observed in the transition between saturated and unsaturated zones. Maximal gas pressures at the galleries wall are about 7 MPa, but they are

strongly dependent on the retention curve of the material. The large drainage at the access gallery wall affects the water pressures in both the concrete and the bentonite plugs.

The comparison of the gas and water profiles in argillite or in the different plugs shows that the mechanical deformations (with elastoplasticity in argillite or nonlinear behaviour in the bentonite plug) are limited on water and gas distributions. The influence of the fluid transfers on the mechanical behaviour is also limited. For instance, swelling pressure in the bentonite plug follows the gas and water evolutions, but it is not influenced significantly by the gas injection. Other strong coupling effects (e.g. permeability variation with damage, complex mechanical laws or retention curves evolution) can possibly influence gas transfers around the repository system and should be studied in the future.

REFERENCES

[1] Ortiz, L., G. Volckaert, D. Mallants. Gas Penetration and Migration in Boom Clay, a Potential Host Rock Formation for Nuclear Waste Storage. *Eng. Geol.*, **64** (2002), 287–296.

[2] Volckaert, G., L. Ortiz, P. De Canniere, M. Put, S. T. Horseman, J. F. Harrington, V. Fioravante, M. Impey. MEGAS: Modelling and Experiments on Gas Migration in Repository Host Rocks, Final report phase 1, Eur. Comm., [Rep.] EUR 16235 EN, 1995.

[3] Horseman, S. T., J. F. Harrington, P. Sellin. Gas Migration in Clay Barriers. *Eng. Geol.*, **54** (1999), 139-149.

[4] Delahaye, C. H., E. E. Alonso. Soil Heterogeneity and Preferential Paths for Gas Migration. *Eng. Geol.,* **64** (2002), 251–271.

[5] ANDRA (Agence Nationale de Gestion des déchets Radioactifs). Référentiel des matériaux d'un stockage de déchets à haute activité et à vie longue. Tome 1: Matériaux à base d'argiles gonflantes, ANDRA 276, 2005, ISBN : 2-916162-12-7, Available from: `http://www.andra.fr`.

[6] ANDRA (Agence Nationale de Gestion des déchets Radioactifs). Référentiel des du site de Meuse/Haute-Marne. Tome 2 : Caractérisation comportementale du milieu géologique sous perturbation, ANDRA 273, 2005, ISBN: 2-916162-06-2, Available from: `http://www.andra.fr`.

[7] Panday, S., M. Y. Corapcioglu. Reservoir Transport Equations by Compositional Approach. *Transport Porous Med.*, **4** (1957), 369–393.

[8] Olivella, S., J., Carrera, A. Gens, E. E. Alonso. Nonisothermal Multiphase Flow of Brine and Gas Through Saline Media. *Transport Porous Med.*, **15** (1994), 271–293.

[9] Philip, J. R., D. A. de Vries. Moisture Movement in Porous Materials under Temperature Gradients. *EOS Trans. AGU*, **38** (1957), No. 2, 222–232.

[10] Weast, R. C. In: Handbook of Chemistry and Physics, **51** (Ed. CRC Press), Cleveland, 1971.

[11] Bemer, E., P. Longuemare, O. Vincke. Poroelastic Parameters of Meuse/Haute Marne Argillites: Effect of Loading and Saturation States. *Appl. Clay Sci.*, **26** (2004), 359–366.

[12] van Genuchten, M. Th. A Closed-Form Equation for Predicting the Hydraulic Conductivity of Unsaturated Soils. *Soil Sci. Soc. Am.*, **44** (1984), 892–898.

[13] Biot, M. A. General Theory of Three-dimensional Consolidation. *J. Appl. Phys.*, **12** (1941), 155–164.

[14] Coussy, O. In: Poromechanics (Ed. Wiley), London, 2004.

[15] Nuth, M., L. Laloui. Effective Stress Concept in Unsaturated Soils: Clarification and Validation of a Unified Framework. *Int. J. Numer. Anal. Meth. Geomech.*, (2007), doi: 10.1002/nag.645

[16] Alonso, E. E., A. Gens, A., Josa. A Constitutive Model for Partially Saturated Soils. *Geotechnique*, **40** (1990), 405-430.

[17] Collin, F., X. L. Li, J. P. Radu, R. Charlier. Thermo-Hydro-Mechanical Coupling in Clay Barriers. *Eng. Geol.*, **64** (2002), 179–193.